

Squark Loop Correction to $W^\pm H^\mp$ Associated Hadroproduction

A. A. Barrientos Bendejú¹ and B. A. Kniehl^{2,*}

¹ II. Institut für Theoretische Physik, Universität Hamburg,
Luruper Chaussee 149, 22761 Hamburg, Germany

² Max-Planck-Institut für Physik (Werner-Heisenberg-Institut),
Föhringer Ring 6, 80805 Munich, Germany

Abstract

We study the squark loop correction to $W^\pm H^\mp$ associated hadroproduction via gluon-gluon fusion within the minimal supersymmetric extension of the standard model. We list full analytic results and quantitatively analyze the resulting shift in the cross section at the CERN Large Hadron Collider assuming a supergravity-inspired scenario.

PACS numbers: 12.60.Fr, 12.60.Jv, 13.85.-t

*Permanent address: II. Institut für Theoretische Physik, Universität Hamburg, Luruper Chaussee 149, 22761 Hamburg, Germany.

1 Introduction

The search for Higgs bosons will be among the prime tasks of the CERN Large Hadron Collider (LHC) [1]. While the standard model (SM) contains one complex Higgs doublet, from which one neutral CP-even Higgs boson emerges in the physical particle spectrum after the electroweak symmetry breaking, the Higgs sector of the minimal supersymmetric extension of the SM (MSSM) consists of a two-Higgs-doublet model (2HDM) and accommodates five physical Higgs bosons: the neutral CP-even h^0 and H^0 bosons, the neutral CP-odd A^0 boson, and the charged H^\pm -boson pair. At the tree level, the MSSM Higgs sector has two free parameters, which are usually taken to be the mass m_A of the A^0 boson and the ratio $\tan\beta = v_2/v_1$ of the vacuum expectation values of the two Higgs doublets.

The discovery of the H^\pm bosons would rule out the SM and, at the same time, give strong support to the MSSM. The main strategies for the H^\pm -boson search at the LHC were summarized in Refs. [1,2]. Depending on the H^\pm -boson mass m_H , the dominant mechanism of single H^\pm -boson hadroproduction are $gg, q\bar{q} \rightarrow t\bar{t}$ followed by $t \rightarrow bH^+$ [1], $g\bar{b} \rightarrow \bar{t}H^+$ [3], $gg \rightarrow \bar{t}bH^+$ [4], and $qb \rightarrow q'bH^+$ [5] together with their charge-conjugate counterparts. The hadroproduction of H^+H^- pairs proceeds at tree level via $q\bar{q}$ annihilation, $q\bar{q} \rightarrow H^+H^-$, where $q = u, d, s, c$ [6], and b [7], and at the one-loop level via gg fusion, $gg \rightarrow H^+H^-$, which is mediated by quark [7,8,9] and squark loops [7,9]. The suppression of the gg -fusion cross section by two powers of the strong-coupling constant α_s relative to the one of $q\bar{q}$ annihilation is partly compensated at multi-TeV hadron colliders by the overwhelming gluon luminosity.

An interesting alternative is to produce H^\pm bosons in association with W^\mp bosons, so that the leptonic decays of the latter may serve as a trigger for the H^\pm -boson search. The dominant partonic subprocesses of $W^\pm H^\mp$ associated production are $b\bar{b} \rightarrow W^\pm H^\mp$ at the tree level and $gg \rightarrow W^\pm H^\mp$ at one loop, which were investigated for vanishing bottom-quark mass m_b and small values of $\tan\beta$ ($0.3 \leq \tan\beta \leq 2.3$) in Ref. [10] and recently, without these restrictions, in Refs. [2,11]. A careful signal-versus-background analysis, based on the analytic results of Ref. [2], was recently reported in Ref. [12]. So far, only the quark loop contribution to $gg \rightarrow W^\pm H^\mp$ was considered [2,10,11]. The purpose of this paper is to provide, in analytic form, the supersymmetric contribution to this partonic subprocess, which is induced by virtual squarks through the Feynman diagrams depicted in Fig. 1. Furthermore, we wish to quantitatively study its influence on the cross section of the inclusive reaction $pp \rightarrow W^\pm H^\mp + X$ at the LHC. We recall that, in the case of $pp \rightarrow H^+H^- + X$, the supersymmetric correction to the gg -fusion cross section can be as large as +50% [7]. *A priori*, one expects to encounter a similar situation for $pp \rightarrow W^\pm H^\mp + X$.

In order to reduce the number of unknown supersymmetric input parameters, we adopt a scenario where the MSSM is embedded in a grand unified theory (GUT) involving supergravity (SUGRA) [13]. The MSSM thus constrained is characterized by the following parameters at the GUT scale, which come in addition to $\tan\beta$ and m_A : the universal scalar mass m_0 , the universal gaugino mass $m_{1/2}$, the trilinear Higgs-sfermion coupling A , the

bilinear Higgs coupling B , and the Higgs-higgsino mass parameter μ . Notice that m_A is then not an independent parameter anymore, but it is fixed through the renormalization group equation. The number of parameters can be further reduced by making additional assumptions. Unification of the τ -lepton and b -quark Yukawa couplings at the GUT scale leads to a correlation between m_t and $\tan\beta$. Furthermore, if the electroweak symmetry is broken radiatively, then B and μ are determined up to the sign of μ . Finally, it turns out that the MSSM parameters are nearly independent of the value of A , as long as $|A| \lesssim 500$ GeV at the GUT scale.

This paper is organized as follows. In Sec. 2, we list the helicity amplitudes of the partonic subprocess $gg \rightarrow W^- H^+$ involving virtual squarks. In Sec. 3, we present quantitative predictions for the inclusive cross section of $pp \rightarrow W^\pm H^\mp + X$ at the LHC adopting the SUGRA-inspired MSSM. Sec. 4 contains our conclusions.

2 Analytic Results

In this section, we express the $gg \rightarrow W^- H^+$ helicity amplitudes involving one closed squark loop in terms of the standard scalar two-, three-, and four-point functions,

$$\begin{aligned}
B_0(p_1^2, m_0^2, m_1^2) &= \int \frac{d^D q}{i\pi^2} \frac{1}{(q^2 - m_0^2 + i\epsilon) [(q + p_1)^2 - m_1^2 + i\epsilon]}, \\
C_0(p_1^2, (p_2 - p_1)^2, p_2^2, m_0^2, m_1^2, m_2^2) \\
&= \int \frac{d^D q}{i\pi^2} \frac{1}{(q^2 - m_0^2 + i\epsilon) [(q + p_1)^2 - m_1^2 + i\epsilon] [(q + p_2)^2 - m_2^2 + i\epsilon]}, \\
D_0(p_1^2, (p_2 - p_1)^2, (p_3 - p_2)^2, p_3^2, p_2^2, (p_3 - p_1)^2, m_0^2, m_1^2, m_2^2, m_3^2) \\
&= \int \frac{d^D q}{i\pi^2} \frac{1}{(q^2 - m_0^2 + i\epsilon) [(q + p_1)^2 - m_1^2 + i\epsilon] [(q + p_2)^2 - m_2^2 + i\epsilon] [(q + p_3)^2 - m_3^2 + i\epsilon]},
\end{aligned} \tag{1}$$

where D is the space-time dimensionality. The B_0 function is ultraviolet (UV) divergent in the physical limit $D \rightarrow 4$, while the C_0 and D_0 functions are UV finite in this limit. We evaluate the B_0 , C_0 , and D_0 functions numerically with the aid of the program package FF [14]. To simplify notation, we introduce the abbreviations $C_{ijk}^{ab}(c) = C_0(a, b, c, m_i^2, m_j^2, m_k^2)$ and $D_{ijkl}^{abcd}(e, f) = D_0(a, b, c, d, e, f, m_i^2, m_j^2, m_k^2, m_l^2)$.

We work in the MSSM adopting the Feynman rules from Ref. [15]. For each quark flavor q there is a corresponding squark flavor \tilde{q} , which comes in two mass eigenstates $i = 1, 2$. In the following, up- and down-type squark flavors are generically denoted by \tilde{t} and \tilde{b} , respectively. The masses $m_{\tilde{q}_i}$ of the squarks and their trilinear couplings $g_{W^- \tilde{t}_i \tilde{b}_j}$, $g_{h^0 \tilde{q}_i \tilde{q}_j}$, $g_{H^0 \tilde{q}_i \tilde{q}_j}$, and $g_{H^\pm \tilde{t}_i \tilde{b}_j}$ to the W^- , h^0 , H^0 , and H^\pm bosons are defined in Eqs. (A.5)

and (A.9) of Ref. [16] and in Eq. (A.2) of Ref. [7], respectively.¹ Furthermore, we have

$$\begin{aligned} g_{W^-H^+h^0} &= -\frac{\cos(\alpha - \beta)}{2}, \\ g_{W^-H^+H^0} &= -\frac{\sin(\alpha - \beta)}{2}, \end{aligned} \quad (2)$$

where α is the mixing angle that rotates the weak CP-even Higgs eigenstates into the mass eigenstates h^0 and H^0 .

Calling the four-momenta of the two gluons and the W boson p_a , p_b , and p_W , respectively, we define the partonic Mandelstam variables as $s = (p_a + p_b)^2$, $t = (p_a - p_W)^2$, and $u = (p_b - p_W)^2$. Furthermore, we introduce the following short-hand notations: $w = m_W^2$, $h = m_H^2$, $d = t - u$, $t_1 = t - w$, $t_2 = t - h$, $u_1 = u - w$, $u_2 = u - h$, $N = tu - wh$, $\lambda = s^2 + w^2 + h^2 - 2(sw + wh + hs)$, and $q = m_{t_i}^2 - m_{b_j}^2$. We label the helicity states of the two gluons and the W boson in the partonic center-of-mass (c.m.) frame by $\lambda_a = -1/2, 1/2$, $\lambda_b = -1/2, 1/2$, and $\lambda_W = -1, 0, 1$.

The relevant Feynman diagrams are depicted in Fig. 1. In analogy to the quark case, we refer to the diagrams involving a neutral Higgs boson in the s channel as triangle diagrams. In contrast to the quark case, the diagrams involving the A^0 boson add up to zero. The residual diagrams are regarded to be of the box type. The helicity amplitudes of the squark triangle contribution read

$$\begin{aligned} \tilde{\mathcal{M}}_{\lambda_a \lambda_b 0}^\Delta &= 4\sqrt{\lambda}(1 + \lambda_a \lambda_b) \sum_{\tilde{q}} \sum_i \left(\frac{g_{W^-H^+h^0} g_{h^0 \tilde{q}_i \tilde{q}_i}}{s - m_{h^0}^2 + im_{h^0} \Gamma_{h^0}} + \frac{g_{W^-H^+H^0} g_{H^0 \tilde{q}_i \tilde{q}_i}}{s - m_{H^0}^2 + im_{H^0} \Gamma_{H^0}} \right) \\ &\quad \times \left[1 + 2m_{\tilde{q}_i}^2 C_{\tilde{q}_i \tilde{q}_i \tilde{q}_i}^{00}(s) \right], \\ \tilde{\mathcal{M}}_{\lambda_a \lambda_b \pm 1}^\Delta &= 0, \end{aligned} \quad (3)$$

where Γ_{h^0} and Γ_{H^0} are the total decay widths of the h^0 and H^0 bosons, respectively. In this case, the W boson can only be longitudinally polarized because it couples to two Higgs bosons. As for the squark box contribution, all twelve helicity amplitudes contribute. Due to Bose² and weak-isospin symmetry, they are related by

$$\begin{aligned} \tilde{\mathcal{M}}_{\lambda_a \lambda_b \lambda_W}^\square(t, u, m_{t_i}^2, m_{b_j}^2) &= (-1)^{\lambda_W} \tilde{\mathcal{M}}_{\lambda_b \lambda_a \lambda_W}^\square(u, t, m_{t_i}^2, m_{b_j}^2), \\ \tilde{\mathcal{M}}_{\lambda_a \lambda_b \lambda_W}^\square(t, u, m_{t_i}^2, m_{b_j}^2) &= -\tilde{\mathcal{M}}_{-\lambda_a - \lambda_b - \lambda_W}^\square(t, u, m_{b_j}^2, m_{t_i}^2), \end{aligned} \quad (4)$$

respectively. Keeping $\lambda_W = \pm 1$ generic, we thus only need to specify four expressions. These read:

$$\tilde{\mathcal{M}}_{++0}^\square = \frac{4}{s\sqrt{\lambda}} \sum_{(\tilde{t}, \tilde{b})} \sum_{i,j} g_{W^- \tilde{t}_i \tilde{b}_j} g_{H^+ \tilde{t}_i \tilde{b}_j} \left[\tilde{F}_{++}^0 + (t \leftrightarrow u) \right],$$

¹In Ref. [16], $m_{\tilde{q}_i}$ and $g_{W^- \tilde{t}_i \tilde{b}_j}$ are called $M_{\tilde{Q}a}$ and \tilde{V}_{UaDb}^W/g , respectively.

²Notice that the interchange of t and u also affects the representation of the W -boson polarization four-vector through its dependence on the angle between the three-momenta of gluon a and the W boson. This explains the sign factor in the first line of Eq. (4), which is not expected from pure Bose symmetry.

$$\begin{aligned}
\tilde{\mathcal{M}}_{+-0}^{\square} &= \frac{4}{N\sqrt{\lambda}} \sum_{(\tilde{t}, \tilde{b})} \sum_{i,j} g_{W-\tilde{t}_i \tilde{b}_j} g_{H+\tilde{t}_i \tilde{b}_j} \left[\tilde{F}_{+-}^0 - (m_{\tilde{t}_i}^2 \leftrightarrow m_{\tilde{b}_j}^2) \right], \\
\tilde{\mathcal{M}}_{++\lambda_w}^{\square} &= \frac{m_W}{\sqrt{N}} \left(\frac{2}{s} \right)^{3/2} \sum_{(\tilde{t}, \tilde{b})} \sum_{i,j} g_{W-\tilde{t}_i \tilde{b}_j} g_{H+\tilde{t}_i \tilde{b}_j} \left[\left(\frac{\tilde{F}_{++}^1}{\sqrt{\lambda}} + \lambda_W \tilde{F}_{++}^2 \right) - (t \leftrightarrow u) \right], \\
\tilde{\mathcal{M}}_{+-\lambda_w}^{\square} &= \frac{m_W}{\sqrt{s}} \left(\frac{2}{N} \right)^{3/2} \sum_{(\tilde{t}, \tilde{b})} \sum_{i,j} g_{W-\tilde{t}_i \tilde{b}_j} g_{H+\tilde{t}_i \tilde{b}_j} \left[\left(\frac{\tilde{F}_{+-}^1}{\sqrt{\lambda}} + \lambda_W \tilde{F}_{+-}^2 \right) - (m_{\tilde{t}_i}^2 \leftrightarrow m_{\tilde{b}_j}^2) \right], \quad (5)
\end{aligned}$$

where $\sum_{(\tilde{t}, \tilde{b})}$ denotes the sum over squark generations and

$$\begin{aligned}
\tilde{F}_{++}^0 &= 2s(t_1 + u_1) \left[m_{\tilde{b}_j}^2 C_{\tilde{b}_j \tilde{b}_j \tilde{b}_j}^{00}(s) - m_{\tilde{t}_i}^2 C_{\tilde{t}_i \tilde{t}_i \tilde{t}_i}^{00}(s) \right] \\
&\quad + [wd - q(t_1 + u_1)] \left[t_2 C_{\tilde{b}_j \tilde{t}_i \tilde{t}_i}^{h0}(t) + t_1 C_{\tilde{t}_i \tilde{b}_j \tilde{b}_j}^{w0}(t) \right] \\
&\quad - [wd + q(t_1 + u_1)] \left[t_2 C_{\tilde{t}_i \tilde{b}_j \tilde{b}_j}^{h0}(t) + t_1 C_{\tilde{b}_j \tilde{t}_i \tilde{t}_i}^{w0}(t) \right] \\
&\quad - [wd - q(t_1 + u_1)] \left[N + s(m_{\tilde{b}_j}^2 + m_{\tilde{t}_i}^2) \right] D_{\tilde{b}_j \tilde{t}_i \tilde{t}_i \tilde{b}_j}^{h0w0}(t, u) \\
&\quad + 2sm_{\tilde{b}_j}^2 [w(t_2 + u_2) + q(t_1 + u_1)] D_{\tilde{b}_j \tilde{t}_i \tilde{b}_j \tilde{b}_j}^{hw00}(s, t) \\
&\quad - 2sm_{\tilde{t}_i}^2 [w(t_2 + u_2) - q(t_1 + u_1)] D_{\tilde{t}_i \tilde{b}_j \tilde{t}_i \tilde{t}_i}^{hw00}(s, t), \\
\tilde{F}_{+-}^0 &= s(t + u - 2q) [w(t_2 + u_2) + q(t_1 + u_1)] C_{\tilde{b}_j \tilde{b}_j \tilde{b}_j}^{00}(s) \\
&\quad - t_2 \{ tw(t_2 + u_2) - q[t(t + 3u) - 2w(t + u) - 2N] \} C_{\tilde{b}_j \tilde{t}_i \tilde{t}_i}^{h0}(t) \\
&\quad - u_2 \{ uw(t_2 + u_2) - q[u(3t + u) - 2w(t + u) - 2N] \} C_{\tilde{b}_j \tilde{t}_i \tilde{t}_i}^{h0}(u) \\
&\quad - t_1 \{ tw(t_2 + u_2) - q[t(d + 4u_1) - 2N] \} C_{\tilde{b}_j \tilde{t}_i \tilde{t}_i}^{w0}(t) \\
&\quad - u_1 \{ uw(t_2 + u_2) + q[u(d - 4t_1) + 2N] \} C_{\tilde{b}_j \tilde{t}_i \tilde{t}_i}^{w0}(u) \\
&\quad - (d^2 + 2N) [w(t_2 + u_2) + q(t_1 + u_1)] C_{\tilde{b}_j \tilde{t}_i \tilde{b}_j}^{hw}(s) \\
&\quad + [wd - q(t_1 + u_1)] \left[N(m_{\tilde{b}_j}^2 + m_{\tilde{t}_i}^2) + sq^2 \right] D_{\tilde{b}_j \tilde{t}_i \tilde{t}_i \tilde{b}_j}^{h0w0}(t, u) \\
&\quad - [w(t_2 + u_2) + q(t_1 + u_1)] \left[st(t - 2m_{\tilde{t}_i}^2) - 2t_1 t_2 m_{\tilde{b}_j}^2 + sq^2 \right] D_{\tilde{b}_j \tilde{t}_i \tilde{b}_j \tilde{b}_j}^{hw00}(s, t) \\
&\quad - [w(t_2 + u_2) + q(t_1 + u_1)] \left[su(u - 2m_{\tilde{t}_i}^2) - 2u_1 u_2 m_{\tilde{b}_j}^2 + sq^2 \right] D_{\tilde{b}_j \tilde{t}_i \tilde{b}_j \tilde{b}_j}^{hw00}(s, u), \\
\tilde{F}_{++}^1 &= -2s^2 d \left[m_{\tilde{b}_j}^2 C_{\tilde{b}_j \tilde{b}_j \tilde{b}_j}^{00}(s) - m_{\tilde{t}_i}^2 C_{\tilde{t}_i \tilde{t}_i \tilde{t}_i}^{00}(s) \right] \\
&\quad + [N(t_1 + u_1) + sdq] \left[t_2 C_{\tilde{b}_j \tilde{t}_i \tilde{t}_i}^{h0}(t) + t_1 C_{\tilde{t}_i \tilde{b}_j \tilde{b}_j}^{w0}(t) \right] \\
&\quad - [N(t_1 + u_1) - sdq] \left[t_2 C_{\tilde{t}_i \tilde{b}_j \tilde{b}_j}^{h0}(t) + t_1 C_{\tilde{b}_j \tilde{t}_i \tilde{t}_i}^{w0}(t) \right] \\
&\quad - \left[N + s(m_{\tilde{b}_j}^2 + m_{\tilde{t}_i}^2) \right] [N(t_1 + u_1) + sdq] D_{\tilde{b}_j \tilde{t}_i \tilde{t}_i \tilde{b}_j}^{h0w0}(t, u) \\
&\quad + 2s^2 m_{\tilde{b}_j}^2 [2N + d(t - q)] D_{\tilde{b}_j \tilde{t}_i \tilde{b}_j \tilde{b}_j}^{hw00}(s, t) - 2s^2 m_{\tilde{t}_i}^2 [2N + d(t + q)] D_{\tilde{t}_i \tilde{b}_j \tilde{t}_i \tilde{t}_i}^{hw00}(s, t), \\
\tilde{F}_{++}^2 &= (N - sq) \left[t_2 C_{\tilde{b}_j \tilde{t}_i \tilde{t}_i}^{h0}(t) - t_1 C_{\tilde{b}_j \tilde{t}_i \tilde{t}_i}^{w0}(t) \right] - (N + sq) \left[t_2 C_{\tilde{t}_i \tilde{b}_j \tilde{b}_j}^{h0}(t) - t_1 C_{\tilde{t}_i \tilde{b}_j \tilde{b}_j}^{w0}(t) \right] \\
&\quad - \left[N^2 + 2sN(m_{\tilde{b}_j}^2 + m_{\tilde{t}_i}^2) + s^2 q^2 \right] D_{\tilde{b}_j \tilde{t}_i \tilde{t}_i \tilde{b}_j}^{h0w0}(t, u),
\end{aligned}$$

$$\begin{aligned}
\tilde{F}_{+-}^1 &= 2sdNB_0 \left(s, m_{b_j}^2, m_{\tilde{b}_j}^2 \right) + s^2 d \left[t^2 + u^2 + 2N - 2q(t+u) + 2q^2 \right] C_{\tilde{b}_j \tilde{b}_j \tilde{t}_i}^{00}(s) \\
&\quad - t_2 \{ st(td + 2N) + q[d(2st + 3N) - 2N(2t_1 + t_2)] \} C_{\tilde{b}_j \tilde{t}_i \tilde{t}_i}^{h0}(t) \\
&\quad - u_2 \{ su(ud - 2N) + q[d(2su + 3N) + 2N(2u_1 + u_2)] \} C_{\tilde{b}_j \tilde{t}_i \tilde{t}_i}^{h0}(u) \\
&\quad - t_1 \{ st(td + 2N) + q[d(2st + N) - 2t_2 N] \} C_{\tilde{b}_j \tilde{t}_i \tilde{t}_i}^{w0}(t) \\
&\quad - u_1 \{ su(ud - 2N) + q[d(2su + N) + 2u_2 N] \} C_{\tilde{b}_j \tilde{t}_i \tilde{t}_i}^{w0}(u) \\
&\quad - sd(d^2 + 4N)(t + u - 2q) C_{\tilde{b}_j \tilde{t}_i \tilde{b}_j}^{hw}(s) \\
&\quad + [2t_1 N - d(N - sq)] \left[N \left(m_{b_j}^2 + m_{\tilde{t}_i}^2 \right) + sq^2 \right] D_{\tilde{b}_j \tilde{t}_i \tilde{b}_j \tilde{t}_i}^{h0w0}(t, u) \\
&\quad - s[2N + d(t - q)] \left[st^2 + 2Nm_{b_j}^2 - sq(2t - q) \right] D_{\tilde{b}_j \tilde{t}_i \tilde{b}_j \tilde{t}_i}^{hw00}(s, t) \\
&\quad + s[2N - d(u - q)] \left[su^2 + 2Nm_{b_j}^2 - sq(2u - q) \right] D_{\tilde{b}_j \tilde{t}_i \tilde{b}_j \tilde{t}_i}^{hw00}(s, u), \\
\tilde{F}_{+-}^2 &= 2sNB_0 \left(s, m_{b_j}^2, m_{\tilde{b}_j}^2 \right) + s \left[s(t^2 + u^2) + 4Nm_{b_j}^2 - 2sq(t + u - q) \right] C_{\tilde{b}_j \tilde{b}_j \tilde{t}_i}^{00}(s) \\
&\quad - t_2 [st^2 + q(2st + N)] C_{\tilde{b}_j \tilde{t}_i \tilde{t}_i}^{h0}(t) - u_2 [su^2 + q(2su + N)] C_{\tilde{b}_j \tilde{t}_i \tilde{t}_i}^{h0}(u) \\
&\quad - t_1 [st^2 + q(2st + N)] C_{\tilde{b}_j \tilde{t}_i \tilde{t}_i}^{w0}(t) - u_1 [su^2 + q(2su + N)] C_{\tilde{b}_j \tilde{t}_i \tilde{t}_i}^{w0}(u) \\
&\quad - s(d^2 + 2N)(t + u - 2q) C_{\tilde{b}_j \tilde{t}_i \tilde{b}_j}^{hw}(s) \\
&\quad + q \left\{ N \left[N + 2s(m_{b_j}^2 + m_{\tilde{t}_i}^2) \right] + s^2 q^2 \right\} D_{\tilde{b}_j \tilde{t}_i \tilde{b}_j \tilde{t}_i}^{h0w0}(t, u) \\
&\quad - s(t - q) \left[st^2 + 4Nm_{b_j}^2 - sq(2t - q) \right] D_{\tilde{b}_j \tilde{t}_i \tilde{b}_j \tilde{t}_i}^{hw00}(s, t) \\
&\quad - s(u - q) \left[su^2 + 4Nm_{b_j}^2 - sq(2u - q) \right] D_{\tilde{b}_j \tilde{t}_i \tilde{b}_j \tilde{t}_i}^{hw00}(s, u). \tag{6}
\end{aligned}$$

Notice that the UV divergences of \tilde{F}_{+-}^1 and \tilde{F}_{+-}^2 cancel in the expression for $\tilde{\mathcal{M}}_{+-\lambda_W}^\square$ in Eq. (5).

The differential cross section of the partonic subprocess $gg \rightarrow W^- H^+$ is then given by [11]

$$\begin{aligned}
\frac{d\sigma}{dt}(gg \rightarrow W^- H^+) &= \frac{\alpha_s^2(\mu_r) G_F^2 m_W^2}{256(4\pi)^3 s^2} \sum_{\lambda_a, \lambda_b, \lambda_W} \left| \mathcal{M}_{\lambda_a \lambda_b \lambda_W}^\triangle + \mathcal{M}_{\lambda_a \lambda_b \lambda_W}^\square \right. \\
&\quad \left. - \tilde{\mathcal{M}}_{\lambda_a \lambda_b \lambda_W}^\triangle - \tilde{\mathcal{M}}_{\lambda_a \lambda_b \lambda_W}^\square \right|^2, \tag{7}
\end{aligned}$$

where $\alpha_s(\mu_r)$ is the strong-coupling constant at renormalization scale μ_r , G_F is Fermi's constant, and $\mathcal{M}_{\lambda_a \lambda_b \lambda_W}^\triangle$ and $\mathcal{M}_{\lambda_a \lambda_b \lambda_W}^\square$ are the helicity amplitudes of the quark triangle and box contributions, which may be found in Eqs. (1) and (3) of Ref. [11], respectively. The relative minus signs between the quark and squark terms in Eq. (7) compensate for the fact that the Feynman rules underlying Ref. [11] differ from those adopted here. Due to Bose symmetry, the cross section $d\sigma/dt$ of $gg \rightarrow W^- H^+$ is symmetric in t and u . Due to charge-conjugation invariance, it coincides with the one of $gg \rightarrow W^+ H^-$, so that the cross section $d\sigma/dt$ of $gg \rightarrow W^\pm H^\mp$ emerges from the right-hand side of Eq. (7) by multiplication with two. The kinematics of the inclusive reaction $AB \rightarrow W^\pm H^\mp + X$, where A and B are colliding hadrons, is described in Sec. II of Ref. [2]. Its double-differential cross section

$d^2\sigma/dy dp_T$, where y and p_T are the rapidity and transverse momentum of the W boson in the c.m. system of the hadronic collision, may be evaluated from Eq. (2.1) of Ref. [2].

3 Phenomenological Implications

We are now in a position to explore the phenomenological implications of our results. The SM input parameters for our numerical analysis are taken to be $G_F = 1.16639 \cdot 10^{-5} \text{ GeV}^{-2}$, $m_W = 80.419 \text{ GeV}$, $m_Z = 91.1882 \text{ GeV}$, $m_t = 174.3 \text{ GeV}$, and $m_b = 4.6 \text{ GeV}$ [17]. We adopt the lowest-order set CTEQ5L [18] of parton density functions for the proton. We evaluate $\alpha_s(\mu_r)$ from the lowest-order formula [17] with $n_f = 5$ quark flavors and asymptotic scale parameter $\Lambda_{\text{QCD}}^{(5)} = 146 \text{ MeV}$ [18]. We identify the renormalization and factorization scales with the $W^\pm H^\mp$ invariant mass s . For our purposes, it is useful to replace m_A by m_H , the mass of the H^\pm bosons to be produced, in the set of MSSM input parameters. We vary $\tan\beta$ and m_H in the ranges $2.5 < \tan\beta < 38 \approx m_t/m_b$ and $120 \text{ GeV} < m_H < 600 \text{ GeV}$, respectively. As for the GUT parameters, we choose $m_{1/2} = 150 \text{ GeV}$, $A = 0$, and $\mu < 0$, and tune m_0 so as to be consistent with the desired value of m_H . All other MSSM parameters are then determined according to the SUGRA-inspired scenario as implemented in the program package SUSPECT [19]. We do not impose the unification of the τ -lepton and b -quark Yukawa couplings at the GUT scale, which would just constrain the allowed $\tan\beta$ range without any visible effect on the results for these values of $\tan\beta$. We exclude solutions which do not comply with the present experimental lower mass bounds of the sfermions, charginos, neutralinos, and Higgs bosons [20].

We now study $pp \rightarrow W^\pm H^\mp + X$ at the LHC, with c.m. energy $\sqrt{S} = 14 \text{ TeV}$. The fully integrated cross section is considered as a function of m_H for $\tan\beta = 3, 10$, and 30 in Fig. 2(a) and as a function of $\tan\beta$ for $m_H = 150, 300$, and 600 GeV in Fig. 2(b). The combined gg -fusion contribution due to quarks and squarks (solid lines) is compared with the one due to quarks only (dotted lines) [2]. For reference, also the $b\bar{b}$ -annihilation contribution (dashed lines) is shown [2]. We note that the SUGRA-inspired MSSM with our choice of input parameters does not permit $\tan\beta$ and m_H to be simultaneously small, due to the experimental selectron mass lower bound [20]. This explains why the curves for $\tan\beta = 3$ in Fig. 2(a) only start at $m_H \approx 260 \text{ GeV}$ and those for $m_H = 150 \text{ GeV}$ in Fig. 2(b) at $\tan\beta \approx 9$. For large m_H , the experimental m_h lower bound [20] enforces $\tan\beta \gtrsim 2.5$. On the other hand, the experimental lower bounds on the chargino and neutralino masses [20] induce an upper limit on $\tan\beta$, which depends on m_H . We observe from Figs. 2(a) and (b) that the supersymmetric correction to the gg -fusion cross section can be of either sign and have a magnitude of order 10%. It exceeds +10% for small $\tan\beta$ and large m_H , while it almost reaches -10% for medium $\tan\beta$ and small or medium m_H . On the other hand, it is generally small for large $\tan\beta$. We recall that, in the case of $pp \rightarrow H^+ H^- + X$, the supersymmetric correction to the gg -fusion cross section can be as large as +50% [7]. As explained in Ref. [2], the dip in the m_H dependence of the gg -fusion cross section located about $m_H = m_t$ [see Fig. 2(a)] arises from resonating top-

quark propagators in the quark box diagrams. Furthermore, the minima of the curves in Fig. 2(b) close to $\tan\beta \approx \sqrt{m_t/m_b} \approx 6$ may be understood by observing that the average strength of the $H^-\bar{b}t$ coupling, which is proportional to $\sqrt{m_t^2 \cot^2\beta + m_b^2 \tan^2\beta}$, is then minimal [7]. As is the quark case [2], the squark triangle and box contributions are similar in size and destructively interfere with each other, so that their superposition is much smaller than each of them separately. As in the case of $pp \rightarrow H^+H^- + X$ [7], the bulk of the squark contribution comes from the stop and sbottom squarks, while the contributions from the first- and second-generation squarks is greatly suppressed because their couplings to the Higgs bosons are significantly smaller than those of the third-generation squarks and their masses are generally larger than those of lightest stop and sbottom squarks, \tilde{t}_1 and \tilde{b}_1 . We conclude that the suppression of the gg -fusion cross section relative to the one of $b\bar{b}$ annihilation remains after the inclusion of the squark loop contributions.

It is interesting to find out how the kinematic behavior of the gg -fusion cross section is affected by the supersymmetric correction. To that end, we study in Figs. 3(a) and (b) the distributions in the W -boson transverse momentum p_T and rapidity y , respectively, for $\tan\beta = 3, 10, 30$, and $m_H = 300$ GeV. While the y distribution does not exhibit any striking features, we observe that the supersymmetric correction leads to an increase of the p_T distribution by more than 50% at large p_T for medium to large $\tan\beta$. This can be traced to the presence of absorptive parts in the squark loop contribution. In fact, if $p_T > \sqrt{\lambda(4m_{\tilde{q}_i}^2, m_W^2, m_H^2)/(4m_{\tilde{q}_i})}$, then $s > 2m_{\tilde{q}_i}^2$, so that pairs of real \tilde{q}_i squarks can be produced.

For a comparison with future experimental data, the $b\bar{b}$ -annihilation and gg -fusion channels should be combined. From Fig. 2(a), we read off that the total cross section of $pp \rightarrow W^\pm H^\mp + X$ at the LHC is predicted to be approximately 500 fb (20 fb) in the considered MSSM scenario if $\tan\beta = 30$ and $m_H = 150$ GeV ($\tan\beta = 3$ and $m_H = 300$ GeV). If we assume the integrated luminosity per year to be at its design value of $L = 100 \text{ fb}^{-1}$ for each of the two LHC experiments, ATLAS and CMS, then this translates into about 100.000 (4.000) signal events per year.

4 Conclusions

We calculated the squark loop contribution to the partonic subprocess $gg \rightarrow W^\pm H^\mp$ within the MSSM, and analyzed its impact on the inclusive cross section of $pp \rightarrow W^\pm H^\mp + X$ and its distributions in transverse momentum and rapidity at the LHC adopting a SUGRA-inspired scenario. Its inclusion may increase or decrease the integrated gg -fusion cross section by up to 10%, depending on the values $\tan\beta$ and m_H . However, $b\bar{b}$ annihilation remains the dominant mechanism of $W^\pm H^\mp$ associated hadroproduction at the LHC. Should the MSSM be realized in nature, then the $W^\pm H^\mp$ channel will provide a copious source of charged Higgs bosons at the LHC, with an annual yield of up to 100.000 signal events.

Acknowledgements

We thank Stefan Dittmaier for useful communications regarding the sign factor in Eq. (4). B.A.K. thanks the Theory Group of the Werner-Heisenberg-Institut for the hospitality extended to him during a visit when this paper was finalized. The work of A.A.B.B. was supported by the Friedrich-Ebert-Stiftung through Grant No. 219747. The work of B.A.K. was supported in part by the Deutsche Forschungsgemeinschaft through Grant No. KN 365/1-1, by the Bundesministerium für Bildung und Forschung through Grant No. 05 HT9GUA 3, and by the European Commission through the Research Training Network *Quantum Chromodynamics and the Deep Structure of Elementary Particles* under Contract No. ERBFMRX-CT98-0194.

References

- [1] Z. Kunszt and F. Zwirner, Nucl. Phys. **B385**, 3 (1992), and references cited therein.
- [2] A. A. Barrientos Bende-zú and B. A. Kniehl, Phys. Rev. D **59**, 015009 (1998).
- [3] J. F. Gunion, H. E. Haber, F. E. Paige, W.-K. Tung, and S. S. D. Willenbrock, Nucl. Phys. **B294**, 621 (1987); R. M. Barnett, H. E. Haber, and D. E. Soper, Nucl. Phys. **B306**, 697 (1988); F. I. Olness and W.-K. Tung, Nucl. Phys. **B308**, 813 (1988); V. Barger, R. J. N. Phillips, and D. P. Roy, Phys. Lett. B **324**, 236 (1994).
- [4] J. L. Diaz-Cruz and O. A. Sampayo, Phys. Rev. D **50**, 6820 (1994).
- [5] S. Moretti and K. Odagiri, Phys. Rev. D **55**, 5627 (1997).
- [6] E. Eichten, I. Hinchliffe, K. Lane, and C. Quigg, Rev. Mod. Phys. **56**, 579 (1984); **58**, 1065(E) (1986); N. G. Deshpande, X. Tata, and D. A. Dicus, Phys. Rev. D **29**, 1527 (1984).
- [7] A. A. Barrientos Bende-zú and B. A. Kniehl, Nucl. Phys. **B568**, 305 (2000).
- [8] S. S. D. Willenbrock, Phys. Rev. D **35**, 173 (1987); J. Yi, M. Wen-Gan, H. Liang, H. Meng, and Y. Zeng-Hui, J. Phys. G **24**, 83 (1998); A. Krause, T. Plehn, M. Spira, and P. M. Zerwas, Nucl. Phys. **B519**, 85 (1998).
- [9] O. Brein and W. Hollik, Eur. Phys. J. C **13**, 175 (2000).
- [10] D. A. Dicus, J. L. Hewett, C. Kao, and T. G. Rizzo, Phys. Rev. D **40**, 787 (1989).
- [11] A. A. Barrientos Bende-zú and B. A. Kniehl, Phys. Rev. D **61**, 097701 (2000).
- [12] S. Moretti and K. Odagiri, Phys. Rev. D **59**, 055008 (1999).
- [13] A. Djouadi, J. Kalinowski, P. Ohmann, and P. M. Zerwas, Z. Phys. C **74**, 93 (1997), and references cited therein.

- [14] G. J. van Oldenborgh, Comput. Phys. Commun. **66**, 1 (1991).
- [15] J. F. Gunion and H. E. Haber, Nucl. Phys. **B272**, 1 (1986); **B278**, 449 (1986);
J. F. Gunion, H. E. Haber, G. Kane, and S. Dawson, The Higgs Hunter's Guide
(Addison-Wesley, Redwood City, 1990).
- [16] R. Hempfling and B. Kniehl, Z. Phys. C **59**, 263 (1993).
- [17] Particle Data Group, D. E. Groom *et al.*, Eur. Phys. J. C **15**, 1 (2000).
- [18] CTEQ Collaboration, H. L. Lai *et al.*, Eur. Phys. J. C **12**, 375 (2000).
- [19] A. Djouadi, J.-L. Kneur, and G. Moultaka, Report No. PM/98-27 and GDR-S-017
(1998).
- [20] V. Ruhlmann-Kleider, Report No. hep-ex/0001061, January 2000, to be published in
the Proceedings of 19th International Symposium on Lepton and Photon Interactions
at High Energies (LP 99), Stanford, California, 9–14 August 1999.

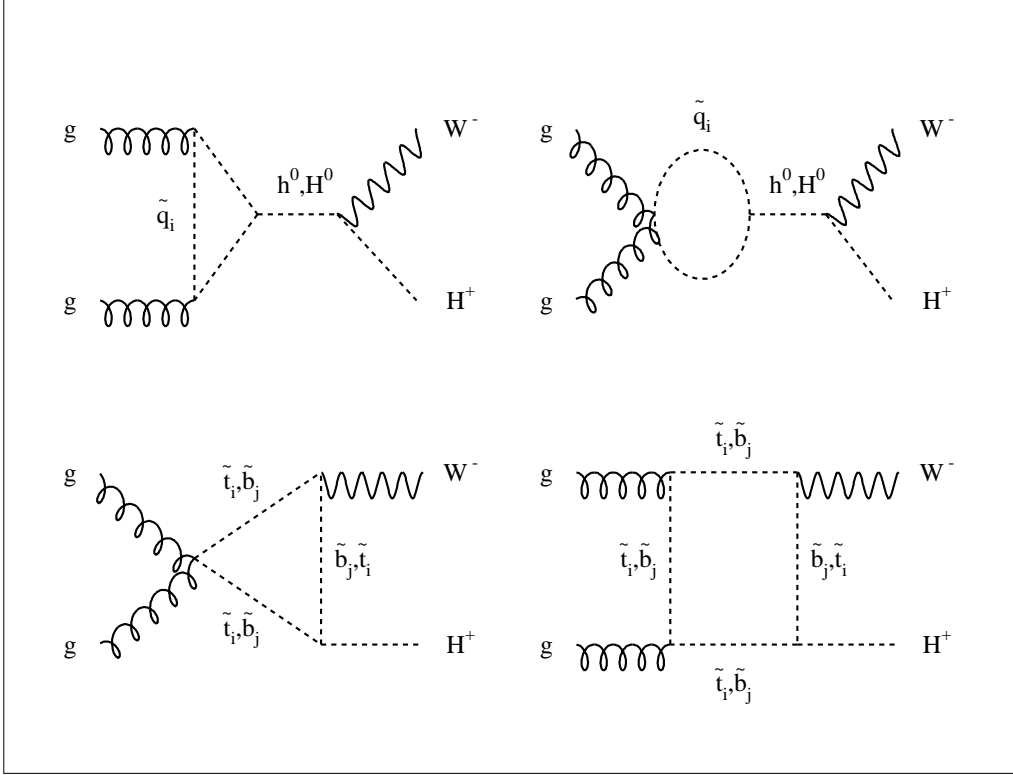


Figure 1: One-loop Feynman diagrams for $gg \rightarrow W^- H^+$ due to virtual squarks in the MSSM.

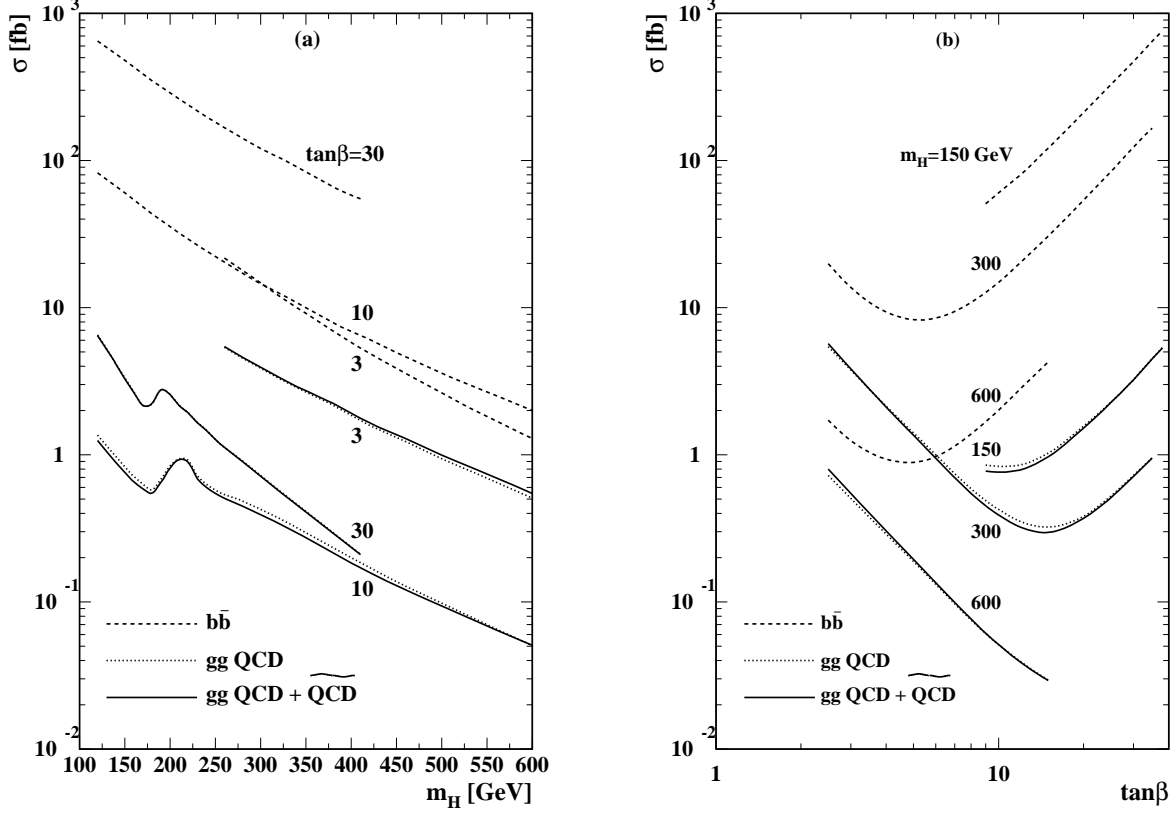


Figure 2: Total cross sections σ (in fb) of $pp \rightarrow W^\pm H^\mp + X$ via $b\bar{b}$ annihilation (dashed lines) and gg fusion (solid lines) at the LHC (a) as functions of m_H for $\tan\beta = 3, 10$, and 30 ; and (b) as functions of $\tan\beta$ for $m_H = 150, 300$, and 600 GeV. For comparison, also the quark loop contribution to gg fusion (dotted lines) is shown.

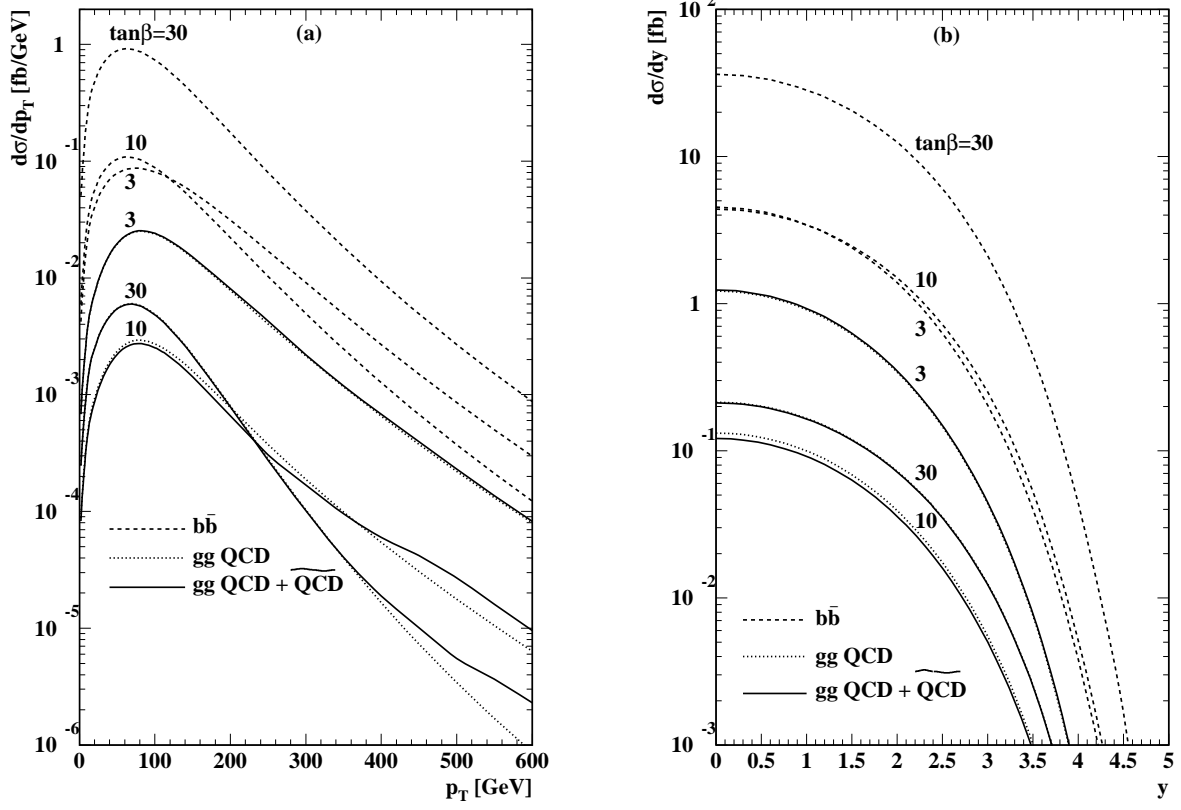


Figure 3: (a) p_T distributions $d\sigma/dp_T$ (in fb/GeV) and (b) y distributions $d\sigma/dy$ (in fb) of $pp \rightarrow W^\pm H^\mp + X$ via $b\bar{b}$ annihilation (dashed lines) and gg fusion (solid lines) at the LHC for $\tan\beta = 3, 10, 30$, and $m_H = 300$ GeV. For comparison, also the quark loop contribution to gg fusion (dotted lines) is shown.